COBEM 2021 26th International Congress of Mechanical Engineering
ABCM Associação Brasileira de Engenharia e Ciências Mecânicas
November 22-26, 2021, Virtual Congress, Brazil

Design of a Platform Aerodynamic Balance for Laminar Wing Force Measurements

João Paulo Eguea
Gabriel Pereira Gouveia da Silva
Fernando Martini Catalano
Department of Aeronautical Engineering, São Carlos School of Engineering, University of São Paulo
joaopeguea@gmail.com
gabriel.gouveia.silva@alumni.usp.br
catalano@sc.usp.br

Abstract. *The aviation industry's goal of designing greener aircraft relies on developing and testing new technologies in fuel, emissions, and noise. Wings designed for extended natural laminar flow (NFL) showed potential for reducing drag and improving aircraft fuel efficiency. The interaction between a laminar wing and a pusher propeller may also beneficially impact the boundary layer stability. Therefore, experimental investigation on the laminar wing and pusher propeller interaction is a possibility for reaching performance improvement in these aviation market sectors. The experimental evaluation of the laminar wing and pusher propeller interaction relies on an accurate lift and drag measurement, demanding the usage of high precision aerodynamic balances. A three-platform aerodynamic balance was developed at the Experimental Aerodynamics Laboratory (LAE) in the Department of Aeronautical Engineering of the University of São Paulo (EESC-USP) to measure aerodynamic forces variations on a laminar wing due to the pusher propeller operation. The chosen design enables measuring lift and drag independently and minimizing the forces and moments cross effect. The balance was designed based on the S-shaped beam theory equations and validation using finite element method (FEM) simulations using Ansys Workbench. The FEM simulations showed that the aerodynamic balance measures the laminar wing forces with less than a 4% difference between applied and measured loads. The fabricated balance will be instrumented, calibrated, and used on the laminar wing and pusher propeller investigation.*

Keywords: *Wind Tunnel Testing, Laminar Flow, Aerodynamic Balance, Finite Element Analysis.*

1. INTRODUCTION

The development of aeronautical projects is an expensive and multidisciplinary task, demanding high expertise personnel. The design process of a new aircraft requires the designers to resort to semi-empirical, computational, and experimental methods for estimating the concept performance. In this context, aircraft aerodynamic design is fundamental to reach project requirements and regulations. Experimental aerodynamics was essential for developing the aerodynamic theory and understanding fluid dynamics phenomena. Further, wind tunnel testing provides valuable and reliable data on different configurations during aircraft design.

Wind tunnel experiments have been used on aircraft design and evaluation since the dawn of aviation (Green and Quest, 2011). The experiments can be used for providing quantitative and qualitative information on different configurations' performance and flow characteristics using a variety of techniques. Forces and moment measurements using aerodynamic balances are widely used for estimating aircraft aerodynamic performance, relying on the flow similarity between a scaled model and the real-size aircraft (Anderson, 1991). This way, force and moment measurements on wind tunnels are a powerful aerodynamic design tool. Despite the great potential from wind tunnel experiments for aerodynamic design, some issues may be highlighted. The limited Reynolds and Mach numbers range achieved on small-scale models are one of its possible drawbacks. However, the development of controlled pressure and temperature test chambers enabled achieving flow similarity for an ample range of flight conditions (Dress and Kilgore, 1988).

The development of more accurate computational fluid dynamics (CFD) tools and more powerful computers enabled faster and reliable simulations. These advances indicate that computational simulations may provide cheaper and faster configuration aerodynamic evaluation than wind tunnel tests. However, it must be highlighted that CFD tools are based on boundary layer and turbulence models and present strong relation between the mesh and solution quality. Further, increasing the CFD model solution quality results in longer wall time for simulations or higher investment to build and maintain clusters. So, despite the CFD simulations' great contributions to aircraft design, they can not fully replace wind tunnel testing. The advances in additive manufacturing also allowed cheaper, faster, and more flexible design and fabrication of wind tunnel models. A deeper discussion on CFD and wind tunnel testing on aircraft design is presented by Pettersson (2006). Wind tunnel testing is used for validating CFD results and aerodynamic evaluation and certification in the preliminary and detailed project phases. Wind tunnel testing is even more relevant to the research and design of innovative solutions. New technologies lack previous data, making it not possible to used data-based estimations and validate simulation results. In this context, wind tunnel measurements provide plenty of information on both flow behavior and aerodynamic performance using simple scaled models and well-established methods, building a database for estimations and simulation validation.

High-quality wind tunnel experiments require proper selection of the facilities and instrumentation (Barlow *et al.*, 1999). In the natural laminar flow wing investigation, the wind tunnel turbulence level must not induce early boundary layer transition on the wing, making this a fundamental parameter for choosing the facilities. Also, the aerodynamic balance must have a measuring range and resolution for detecting variations on the aerodynamic forces and moments due to the changes in the boundary layer transition position. A platform aerodynamic balance was designed at the Experimental Aerodynamics Laboratory (LAE) in the Department of Aeronautical Engineering of the University of São Paulo (EESC-USP) for complying with the requirement for investigating the impact of a pusher propeller on a laminar wing aerodynamic forces.

2. BALANCE CONCEPT

The aerodynamic balance design was based on the three-platform concept developed by Maunsell and Fernandes (1977). This aerodynamic balance enables independent lift and drag measurement, minimizing forces cross-effect. The aerodynamic balance was designed for fitting inside an airfoil-shaped fairing at both wing extremities (Fig. 1). The fairing is fixed to a support structure connected to the turntable, not interacting with the wing and aerodynamic balance, and does interfere with the wing forces measurements. The aerodynamic balance is composed of three platforms and four pairs of sheets (Fig. 2). The aerodynamic balance is turned with the wing model, implying the measurement of the axial (F_x) and normal (F_y) forces.

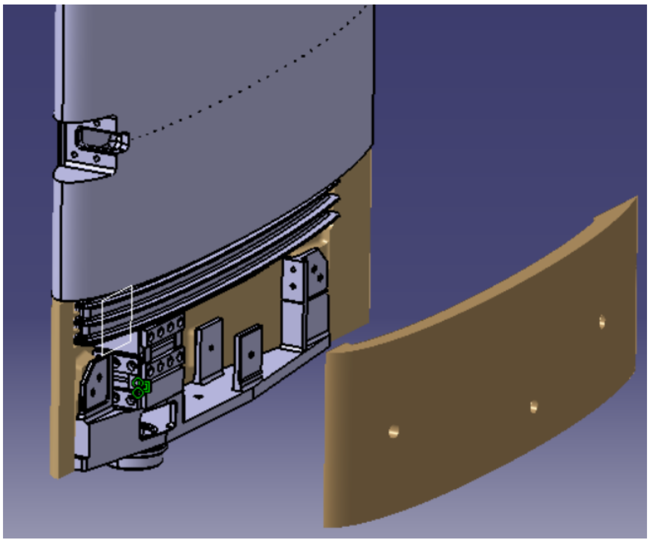

Figure 1. Aerodynamic balance and wing connection drawing

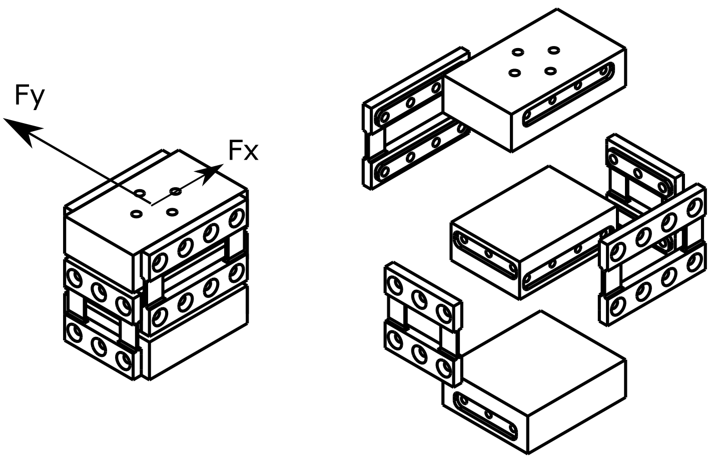

Figure 2. Aerodynamic balance exploded view drawing

The axial and normal forces are measured based on the deformation measurements on the lower and upper pairs of metal sheets, respectively. Two complete bridges are used for measuring each force and the strain gauge positioning and bridge configuration is shown in Figure 3. The following configuration minimizes the forces and moments cross-effect due to the difference in the sheet area moment of inertia (I) in different directions.

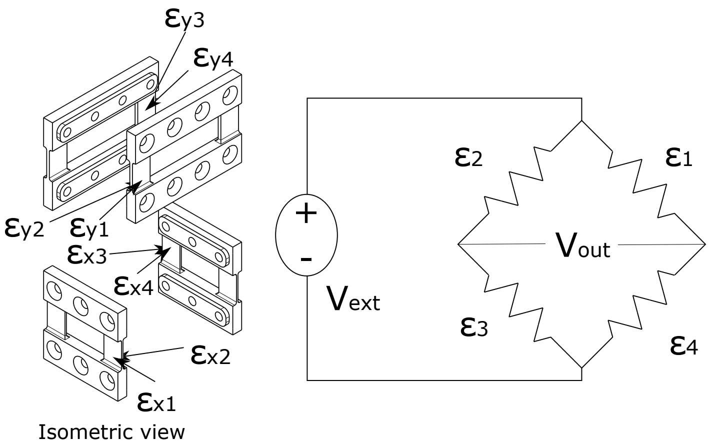

Figure 3. Strain gauges position on metal sheets and bridge configuration

3. BALANCE DESIGN

Initially, the expected aerodynamic loads were estimated based on the wind tunnel operations conditions and airfoil XFoil simulation results. The aluminum 7075 aeronautical alloy was used for the balance fabrication due to its high yield stress (σ_{max}) and low Young's longitudinal modulus (E). The material characteristics and maximum loads are summarized in Table 1.

Table 1. Aerodynamic balance material and loads

Material	E $[MPa]$	σ_{max} $[MPa]$	$F_{x_{max}}$ $[N]$	$F_{y_{max}}$ $[N]$	$M_{y_{max}}$ $[Nm]$
Al-7075	73057	436.2	101.8	368.8	19.1

The balance dimensions were designed based on the Euler-Bernoulli beam theory (Hibbeler, 2016) and the limitations for fitting inside the fairing (Tab. 2). The platforms were assumed to be rigid and the sheets were considered flexible only in the direction normal to its surface. In the present model, the lower platform is assumed to be fixed and the middle and upper are free to move in all directions. The wing aerodynamic forces and moments are transmitted to the balance through four bolts on the upper surface and are assumed to be concentrated on the center of the balance. The free-body diagrams used on the design based on the simplifying hypotheses and constraints are shown in Figures 4 to 7.

Table 2. Aerodynamic balance dimensions

haba $[mm]$	h1 $[mm]$	Lx $[mm]$	Ly $[mm]$	taba $[mm]$	H $[mm]$	hgap $[mm]$
14	20	60	42	5	66	3

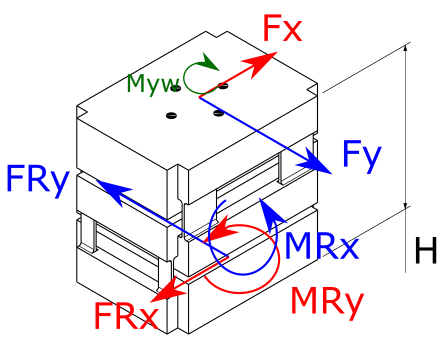

Figure 4. Aerodynamic balance free body diagram

$$\mathbf{F_{Rx}} = \mathbf{F_x} \tag{1}$$

$$\mathbf{F_{Ry}} = \mathbf{F_y} \tag{2}$$

$$\mathbf{M_{Ry}} = \mathbf{F_x\,H + M_y\,W} \tag{3}$$

$$\mathbf{M_{Rx}} = \mathbf{F_y\,H} \tag{4}$$

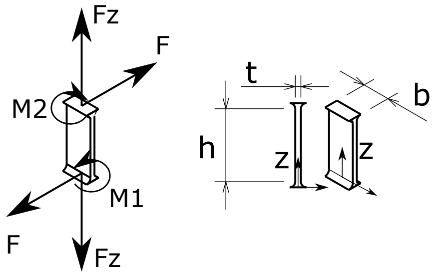

Figure 5. Sheets free body diagram

$$\mathbf{u_{z=0}} = \mathbf{0} \tag{5}$$

$$\theta_{\mathbf{z=0}} = \mathbf{0} \tag{6}$$

$$\theta_{\mathbf{z=h}} = \mathbf{0} \tag{7}$$

$$\mathbf{I} = \frac{\mathbf{bt^3}}{\mathbf{12}} \tag{8}$$

$$\mathbf{E\,I}\,\theta_{\mathbf{i}} = \frac{\mathbf{Fz^2}}{\mathbf{2}} - \frac{\mathbf{Fhz}}{\mathbf{2}} \tag{9}$$

$$\mathbf{E\,I\,u_i} = \frac{\mathbf{Fz^3}}{\mathbf{6}} - \frac{\mathbf{Fhz^2}}{\mathbf{4}} \tag{10}$$

$$\mathbf{M_1} = \mathbf{M_2} = \frac{\mathbf{Fh}}{\mathbf{2}} \tag{11}$$

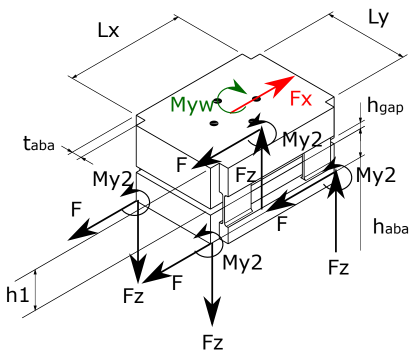

Figure 6. F_x sheet free body diagram for design

$$\mathbf{F} = \frac{\mathbf{F_x}}{\mathbf{4}} \tag{12}$$

$$\mathbf{F_z}\left(\frac{\mathbf{L_x} + \mathbf{t_{aba}}}{\mathbf{2}}\right) = \frac{\mathbf{F_x}}{\mathbf{4}}\left(\mathbf{h_1} + \mathbf{h_{gap}} + \mathbf{h_{aba}}\right) - \mathbf{M_{y2}} \tag{13}$$

$$\mathbf{F_z}\left(\frac{\mathbf{L_x} + \mathbf{t_{aba}}}{\mathbf{2}}\right) = \frac{\mathbf{F_x}}{\mathbf{4}}(\mathbf{h_1} + \mathbf{h_{gap}} + \mathbf{h_{aba}}) - \frac{\mathbf{F_x h}}{\mathbf{8}} \tag{14}$$

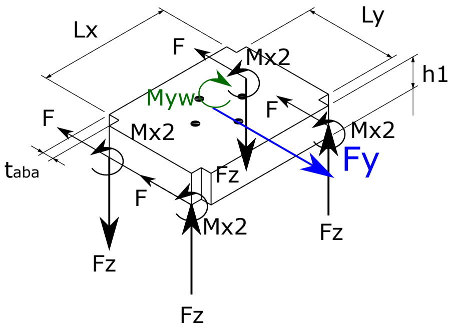

Figure 7. F_y sheet free body diagram for design

$$\mathbf{F} = \frac{\mathbf{F_y}}{\mathbf{4}} \tag{15}$$

$$\mathbf{F_z}\left(\frac{\mathbf{L_y} + \mathbf{t_{aba}}}{\mathbf{2}}\right) = \frac{\mathbf{F_y}\ \mathbf{h_{aba}}}{\mathbf{4}} - \mathbf{M_{y2}} \tag{16}$$

$$\mathbf{F_z}\left(\frac{\mathbf{L_y} + \mathbf{t_{aba}}}{\mathbf{2}}\right) = \frac{\mathbf{F_y}\ \mathbf{h_{aba}}}{\mathbf{4}} - \frac{\mathbf{F_y}\ \mathbf{h}}{\mathbf{8}} \tag{17}$$

Equations 1 to 17 show forces and moments relations and linear and angular displacements calculation. The sheets' dimensions were designed to elastically deform and the security factors (SF) were calculated as shown in Table 3.

Table 3. Sheets dimensions

Direction	t [mm]	b [mm]	h [mm]	SF
x	0.8	10	15	1.67
y	1.5	10	15	1.63

4. RESULTS

The aerodynamic balance was simulated using the Ansys WorkBench static structural finite element analysis (FEA) for estimating the deformations under different load conditions. The mesh and simulation results are shown in Figures 8 to 10.

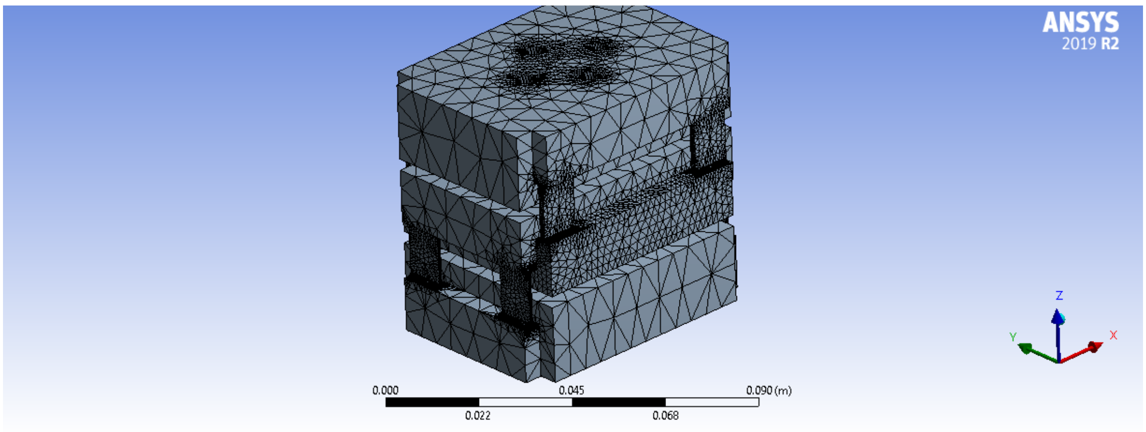

Figure 8. FEA simulation mesh

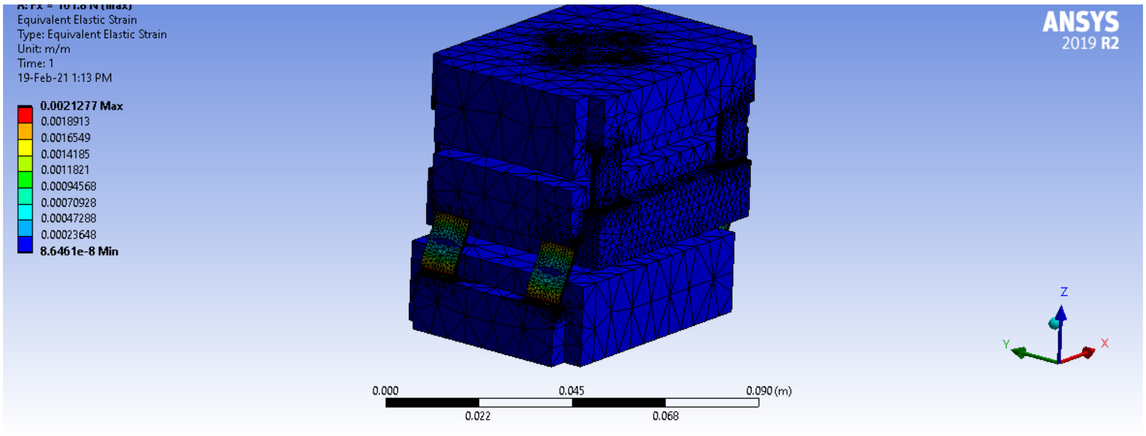

Figure 9. FEA simulations equivalent elastic strain results for $F_x = 101.8N$ and $F_y = 0$

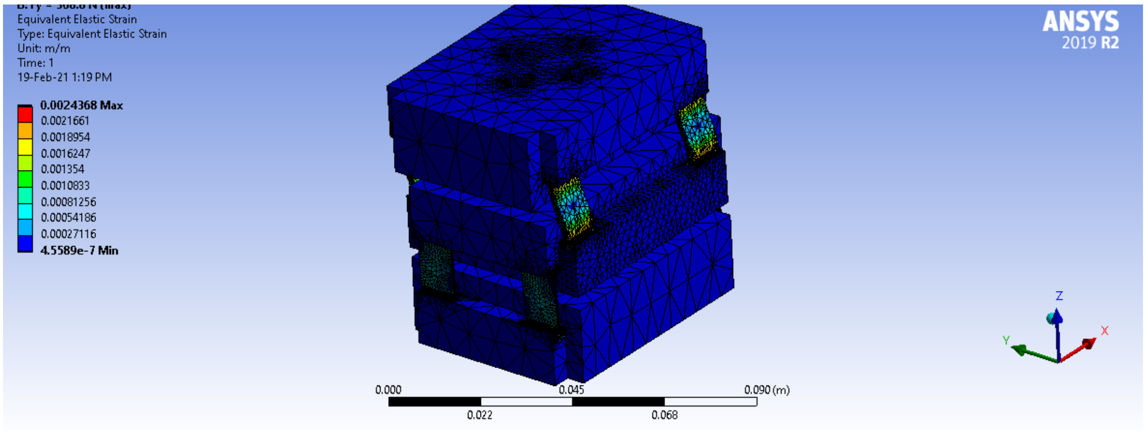

Figure 10. FEA simulations equivalent elastic strain results for $F_x = 0$ and $F_y = 368.8N$

The simulations were performed for estimating the balance response to forces in each direction. The measurement bridge output will be acquired and conditioned using an HBM MCG Plus signal conditioner and a 16-bit National Instruments acquisition system on a PXI. The system measures the total strain (ϵ) based on the strain gauges strain measurements as:

$$\epsilon = \epsilon_1 - \epsilon_2 + \epsilon_3 - \epsilon_4 \quad (18)$$

Where ϵ_i corresponds to the deformation at each strain gauge as shown in Figure 3. The forces inputs and strain outputs were correlated and a calibration constant was calculated for each direction as shown in Table 4.

Table 4. Force and strain correlation

F_x [N]	ϵ_x [$\mu\epsilon$]	F_y [N]	ϵ_y [$\mu\epsilon$]
0.06	0.55	0.06	0.60
20.00	292.27	50.00	260.95
50.00	730.66	100.00	521.91
75.00	1254.71	200.00	1043.81
101.82	1703.48	300.00	1565.71
		368.81	1924.81
$\frac{dF_x}{d\epsilon_x} = 0.06083$		$\frac{dF_y}{d\epsilon_y} = 0.1916$	

Some lift and drag conditions were simulated to verify the balance accuracy, sensitivity, and the forces and moment cross-effects. The weight effect (Case 2) was subtracted from the results as an offset. This procedure is also performed on experiments. The simulation results show that an error smaller than 6% between the applied and measured forces (Tab.

5). This way, the proposed design was efficient in isolating the force measurements in the axial and normal directions. The 16-bit data acquisition system has a voltage output range of $V_{out} = \pm 10V$, resulting in a voltage resolution of $\Delta V = 0.0061V$. This way, considering the maximum deformation output equal to 9 V on both directions, the aerodynamic balance resolution for lift (C_L) and drag (C_D) coefficients measurements are $\Delta C_L = 0.00019$ and $\Delta C_D = 0.00006$, based on the acquisition system specifications. The resolution is sufficient for measuring both lift and drag variations due to changes in the boundary layer transition. The results show that the proposed design is suitable for performing the wind tunnel experiments on the laminar wing and pusher propeller interaction project.

Table 5. Aerodynamic balance pitching moment, wing weight and forces cross-effects results

	Case 1	Case 2	Case 3	Case 4	Case 5	Case 6	Case 7	Case 8
F_x $[N]$	0.00	0.00	90.51	44.73	15.54	1.36	11.53	0.53
F_y $[N]$	0.00	0.00	368.81	272.73	163.31	0.06	73.56	0.35
W $[N]$	0.00	400.00	400.00	400.00	400.00	400.00	400.00	400.00
M_{weight} $[Nm]$	0.00	44.00	444.00	44.00	44.00	44.00	44.00	44.00
M_{yw} $[Nm]$	19.1	0.00	13.36	9.41	9.50	0.00	0.56	0.08
ϵ_x $[\mu\epsilon]$	0.10	5.29	1396.83	694.09	247.69	26.47	182.19	13.88
ϵ_y $[\mu\epsilon]$	0.08	7.97	1752.81	1298.41	780.71	8.32	356.15	9.71
$F_{x_{meas}}$ $[N]$	0.01	0.34	95.79	44.80	15.76	1.38	11.51	0.56
$F_{y_{meas}}$ $[N]$	0.02	1.68	366.96	271.39	162.51	0.07	73.22	0.37
$error_{F_x}$ $[\%]$			-5.84	-0.14	-1.44	-1.61	0.25	-5.30
$error_{F_y}$ $[\%]$			0.50	0.49	0.49	-28.69	0.46	-4.45

5. CONCLUSIONS

Wind tunnel experiments are a powerful tool for evaluating configurations' aerodynamic performance. They provide reliable data on aerodynamic forces and flow characteristics of complex aircraft concepts. However, the quality of the results depends on proper instrumentation and facilities selection. The experiments must achieve a flow similar to the flight conditions and provide accuracy and precision to the measurements. In this context, this work presented the design process and preliminary results obtained on the development of an aerodynamic balance for the testing campaign of the laminar wing and pusher propeller interaction.

A three-platform aerodynamic balance concept was chosen for this purpose. The proposed concept enables measuring both axial (F_x) and normal (F_y) forces independently on a laminar wing model. The theoretical background, used equations, constraints, and expected loads were presented. The Ansys WorkBench static structural finite element analysis (FEA) simulations showed the designed balance achieved the desired accuracy and resolution for the project test campaign.

Future work includes the fabrication and instrumentation of the aerodynamic balance for performing some preliminary evaluation experiments. Further, the three-platform aerodynamic balance concept allows changing the pair of sheets once these elements are bolted to the platforms. This feature enables redesigning these elements if the fabricated balance does not achieve the expected performance and reusing the balance in projects with different loads.

6. RESPONSIBILITY NOTICE

The following text, properly adapted to the number of authors, must be included in the last section of the paper:
The authors are solely responsible for the printed material included in this paper.

7. REFERENCES

Anderson, J., 1991. *Fundamentals of aerodynamics*. McGraw-Hill, New York. ISBN 0070016798.

Barlow, J.B., Rae, W.H. and Pope, A., 1999. *Low-Speed Wind Tunnel Testing*. WILEY. ISBN 0471557749.

Dress, D. and Kilgore, R., 1988. "Cryogenic wind tunnel research: a global perspective". *Cryogenics*, Vol. 28, No. 1, pp. 10–21. doi:10.1016/0011-2275(88)90224-x.

Green, J. and Quest, J., 2011. "A short history of the european transonic wind tunnel ETW". *Progress in Aerospace Sciences*, Vol. 47, No. 5, pp. 319–368. doi:10.1016/j.paerosci.2011.06.002.

Hibbeler, R.C., 2016. *Mechanics of materials*. Pearson, Boston. ISBN 0134319656.

Maunsell, M.G. and Fernandes, O.C., 1977. *Desenvolvimento, construcao e ensaios de uma balanca aerodinamica*. Master's thesis, University of São Paulo.

Pettersson, K., 2006. "Scaling techniques using cfd and wind tunnel measurements for use in aircraft design".